

Determining EGRET's Efficiency Scaling Factors

D. L. Bertsch

11/22/2000

1 Introduction

The efficiency of EGRET changed throughout the mission due largely to the aging of the spark chamber gas, and later in the mission from hardware aging or partial failure. The In-Flight Calibration paper (Esposito et al. 1999, ApJ, 123, 203) discussed the procedures used to determine the time and energy dependence of the scale factors for phases 1 through 4. In short, the scale factors for $E > 100 \text{ MeV}$ were obtained by comparing the diffuse emission for a given viewing period with a so-called 'ideal gas map' that was made by transforming the model of the diffuse emission (Hunter et al. 1997, ApJ, 481, 205) by multiplying factors, GMULT, and offset factors, GBIAS, that were obtained with the LIKE program using a summed map for periods near the start of the mission and immediately after the first three gas exchanges. Similarly, LIKE was used on individual viewing period maps for $E > 100 \text{ MeV}$ to model out the sources and produce GMULT and GBIAS arrays. These were used to transform the same gas model (Hunter et al, 1997) and arrive at an estimate of the residual diffuse emission for that period. Finally, a ratio of the viewing period diffuse to the 'ideal gas map' diffuse was obtained for each pixel in the viewing period map, and a Gaussian fit was done to obtain an estimate of the scale factor and its uncertainty.

The energy dependence was inferred using a similar process for wide energy bands, $30 < E < 100 \text{ MeV}$, $100 < E < 300 \text{ MeV}$, $300 < E < 1000 \text{ MeV}$, and $E > 1000 \text{ MeV}$. These data were then fit with a functional form

- DLB used E^{-2} -weighted means for the ~~the~~ bands

$$S(E, t) = 1.0 + \{2.18 - 0.52 \log_{10}(E)\} \times \{S_{E>100}(t) - 1.0\} \quad (1)$$

The last gas fill was done just before viewing period 4280. Afterward, the efficiency only improved to about the 65% level for $E > 100 \text{ MeV}$, and by the end of the mission, (716 operating days) it had degraded very significantly. The degradation was more severe in the low and moderate energies where gaps in the tracks caused a larger fraction to be rejected.

Table 1. Steps in Analyzing Viewing Period Efficiencies

Process Name	Type	Function
find_sf	PERL	LIKE analysis of > 100 MeV map. Create psf file. Extract Phase 1-3 source-subtracted map.
find_sf_std10	PERL	LIKE analysis of 10 standard energy map using psf file. Extract Phase 1-3 source-subtracted map.
plot_sf	IDL	Generates > 100 MeV efficiency factor. Stores the result.
plot_sf_std10	IDL	Generates the 10 standard energy efficiency factors. Stores the results.

Consequently, the energy dependence became more significant with time so that eq. 1 no longer is an adequate description of the scale factors. Also, a better procedure was needed to be able to track the efficiencies of the standard energy interval to very low levels. This article summarizes modifications to the analysis process on individual viewing periods and discusses the modeling that was done to obtain factors for the standard 10 energy intervals. Finally a brief section is included that discusses the checks that were made to the new process.

2 Viewing Period Analysis

An analysis based on the observed source-subtracted diffuse emission in each of the viewing periods since the last gas refill (starting with VP4280) as compared to the Phase 1-3 source-subtracted diffuse maps was carried out using LIKE as the primary tool. For each viewing period, a LIKE analysis using the $E > 100$ MeV map was done to determine the sources in the field of view. That source list was then used in a LIKE analysis on each of the 10 standard energies to determine the residual flux after the sources had been subtracted. These LIKE analyses were controlled by two scripts. After each script completion, an IDL process was invoked to calculate the observed efficiency and store the results. The names and functions of the four processes are listed in Table 1.

To insure that all of the > 100 MeV maps and 10 standard energy maps were made with the same set of efficiency factors. A full set of the exposure maps was generated in the directory `/data/mozart/dlb/New_maps/Maps`. A Fortran program EXPGEN in that location read a list of names of counts maps and sequentially initiated the INTMAP program. The PERL scripts mentioned above were modified to create a link to the counts map in the same area as the new exposure maps and to look to this location when performing the LIKE analysis.

The four step process required for each viewing period was automated by means of a Fortran program called BATCHEFF in the directory */data/mozart/dlb/Efficiency* where the efficiency analysis was done. This program takes a list of four digit viewing period numbers as input.

The subsections below describe in more detail the four processes of the analysis.

2.1 > 100 MeV Map Analysis

2.1.1 *FIND_SF*

The PERL script *FIND_SF* requires a command line input with a counts file name (without the path) and a number for the desired energy interval (typically 2 when the extension is *.g002* for the > 100 MeV region), e.g., *find_sf counts.vp4280.g002 2*. It then produces a subdirectory, *VPxxxx* where all subsequent output is written. Two LIKE scripts, *like_sf.script* and *stdmap_sf.script* and a LIKE control file *CTL* are generated prior to initiating LIKE.

In the first LIKE session, the environment variable, *\$GMAP_DIR* points to the standard location, */analysis1/data/difmaps/*. A LIKE 'lpms' function is done to generate and save a 'psf' file named 'vpxxxx.psf' (xxxx is the four digit viewing period number.) for $E > 100$ MeV. The *GMULT* and *GBIAS* arrays are also saved and are renamed *vpxxxx.gmult* and *vpxxxx.gbias* by the script. A LIKE 'omg' function is invoked with *GMULT = 1* and *GBIAS = 0* to write out the gas map (diffuse model) as flux, and it is renamed to *vpxxxx.dif*.

Before the second LIKE session is started by the script, the environment variable *\$GMAP_DIR* is set to */home/egret/pxs/DIFFUSE/ANAL/LIKEMAPS/* where the "ideal gas maps" for each map type are stored. This session of LIKE just repeats the 'omg' function with *GMULT = 1* and *GBIAS = 0* to write out the ideal map for the region of the viewing period map. This map is renamed *vpxxxx.std*.

In summary, the important files produced by *find_sf* script in the *./VPxxxx* directory are

	<i>vpxxxx.psf</i>	> 100 MeV psf list for viewing period
	<i>vpxxxx.dif</i>	source-subtracted diffuse map for the viewing
period	<i>vpxxxx.gmult</i>	gmult array map
	<i>vpxxxx.gbias</i>	gbias array map (units of 10^{-5})
	<i>vpxxxx.std</i>	'ideal gas map' for the viewing region

2.1.2 PLOT_SF.PRO

The IDL routine *plot_sf.pro* prompts the user for a four digit viewing period number and expects to find the files discussed in the previous section in a subdirectory named *VPxxxx*. It assumes that the analysis will be done on the $E > 100$ MeV map. (This can be changed by editing the code.) The routine opens the file $\$EGRET_PROGRAMS/sequence/wide.dat$ and looks for an entry for the viewing period being analyzed. If it does not find an entry, it uses the value for the last entry in the table and it prints a message to that effect together with the value it is using. (NOTE: The *wide.dat* table is not used by other software and potentially could be out-of-date causing a erroneous correction to the observed result. The scale factors for wide intervals are generated from the 10 standard values using the program 'genwide' in the directory */home/mozart/dlb/Software/Fort/Wide_E_ScaleFactors*). These scale factors are used to remove the corrections used in generating the exposure and intensity maps so that the final scale factor determination is absolute.

given +
scale factor
ratio chd
#ITS factors ?

The IDL routine forms an intensity map called 'new_map'

$$\text{new_map} = \text{vpxxxx.dif} * \text{vpxxxx.gmult} + \text{vpxxxx.gbias} * 10^{-5} \quad (2)$$

that in reality is equivalent to the observed diffuse map for the > 100 MeV interval for the viewing period. Note that a simpler approach that gives exactly the same result would have been to have LIKE model the sources then set GMULT and GBIAS to 0 using the 'c' subcommand, followed by an abort. Then write out the residual which would be the difference between the total observed flux and the flux from sources. This would be achieved with the LIKE 'omrf' command.

Two ratio analyses are done. In the first (Sreekumar's method), the ratio pixel-by-pixel is formed by

$$\text{ratio} = \text{scalefactor} * \frac{\text{new_map}}{\text{vpxxxx.std}} \quad (3)$$

The term, 'scalefactor' removes the correction used when the exposure maps were created. The Sreekumar method proceeds by forming a distribution of the pixel ratios within 15° of the pointing axis. The mean and standard deviation are output as the new scale factor and uncertainty. The routine also generates plots of the distribution as well as plots of the radial and axial cut distributions.

In some of the shorter viewing periods, the weak statistics in both the viewing period and standard maps give rise to large fluctuations, and the distribution many times is not well represented by a Gaussian. This is even more apparent in analysis of the 10 standard energy intervals that will be discussed below. As an alternative, the other method, which was used exclusively in the final analysis, generates a single value for the ratio

$$\text{ratio} = \text{scalefactor} * \frac{\sum_{15^\circ}(\text{new_map})}{\sum_{15^\circ}(\text{vpxxxx.std})} \quad (4)$$

where the summations are over the central 15° of the field of view.

This second method does not give a measure of the statistical uncertainty, but it can be estimated by the following arguments. For a ratio $R = A/B$, where A and B are independent,

$$\text{var}(R) = R^2 * \left\{ \frac{\text{var}(A)}{A^2} + \frac{\text{var}(B)}{B^2} \right\}$$

In the situation of interest here, the variance of the denominator term (the standard map) is expected to be less than for the numerator term (single viewing period) so that for this case

$$\frac{\text{var}(A)}{B^2} < \text{var}(R) < \frac{2 * \text{var}(A)}{B^2}$$

The variance in the numerator of equation. 4 is variance ^{of} the $\sum_{15^\circ} \text{var}(\text{counts})/\text{exposure}^2$ or $\sum_{15^\circ} \text{new_map}/(\text{exposure})$. Here, exposure refers to the exposure for new_map. Consequently,

$$\text{var}(\text{ratio}) \simeq 2 * \text{scalefactor}^2 * \frac{\sum_{15^\circ} \text{new_map}/\text{exposure}}{(\sum_{15^\circ} \text{vpxxxx.std})^2} \quad (5)$$

Results from both methods were stored for each viewing period analyzed. As will be seen later, they are generally in good agreement. As noted above, the second method was used exclusively in the final analysis.

Finally, 'plot_sf' appends the efficiency for $E > 100$ MeV to a file named 'gt100.table' in the main directory, /data/mozart/dlb/Efficiency. If this file does not exist, it will be created when the first viewing period is analyzed.

2.2 Analysis for the 10 Standard Energy Intervals

A similar pair of processes was developed to determine the scale factors for the 10 standard energy intervals. P. Sreekumar developed the PERL script, *find_sf_std10*

that controls the two LIKE sessions for a given viewing period. A modified version in */data/mozart/dlb/Efficiency* recognizes the coordinate system of the input map and selects the appropriate reference map. It also looks for the maps in the location where the new exposure maps were stored rather than in the standard FITS locations. The companion IDL routine *plot_sf_std10.pro* was written by Bertsch, using much of the same code written by Sreekumar in the > 100 MeV analysis.

2.2.1 FIND_DF_STD10

This PERL script requires a command line input that is the counts file name without its path. Generally, the extension should always be *.g001* although the code does allow for other energy ranges and hence other extensions. This script assumes that the > 100 MeV analysis described above has been done since it will look for an existing subdirectory and a file there named *vpxxxx.psf*.

Rather than using the 'ideal gas maps' as a standard (They have not been made yet for the 10 energy intervals.), the summed phase 1 through 3 maps with sources subtracted are used. These have better statistics than the ideal maps which have a rather restricted time selection. They were created using LIKE with the psf file for the Second EGRET catalog plus the Second Catalog Supplement sources. After a LIKE 'lm' function optimization with fixed locations, the gas model was nulled by setting GMULT and GBIAS to zero and writing out the residual as flux using the LIKE 'omrf' subcommand. The *find_sf_std10* script assumes that these reference maps (or links) exist in the current directory (*/data/mozart/dlb/Efficiency*) and that the reference maps are named *g123_nosrc.g001a*, *g123_nosrc.g001b*, *g123_nosrc.g001c*, ... *g123_nosrc.g001j* where the end letters signify the energy band and the initial letter signifies galactic coordinates. As second set whose initial letter is 'c' for celestial must also exist. A full set of these reference maps are found in */data/mozart/dlb/P123_Maps*.

approximate
catalog
phase 3

For each of the 10 energy intervals, the script creates two LIKE control files, *CTL* and *CTL_res* and two LIKE script files, *like_sf_std10.script* and *stdmap_sf_std10.script* appropriate for that energy, and it proceeds to initiate two LIKE sessions. The first control file and script open the viewing period files of interest and read in the *vpxxxx.psf* file generated in the > 100 MeV processing. The script then performs a LIKE 'lm' optimization, sets GMULT and GBIAS to zero (to nullify the diffuse model), and writes out the residual (difference between the observed flux and the source modeled flux) using the 'omrf' subcommand. These maps are named *vpxxxx.g001[a-j].resflx*. Each letter in the brackets represent one of the 10 energy bands. The second LIKE session for a specific energy region simply extracts the part of the Phase 1-3 map that applies to the viewing period region. This is done reading in the appropriate Phase 1-3 source-subtracted map as the gas map. In this run, no sources are read into the psf, GMULT is set to 1, and GBIAS is set to zero. Then a LIKE 'omg' function writes out the gas map as flux. These maps are named *vpxxxx.g001[a-j].stdresflx*.

2.2.2 PLOT_SF_STD10.PRO

This IDL routine prompts the user for a four digit viewing period number and expects to find the files discussed in the previous section in a subdirectory named VPxxxx. It assumes that the analysis will be done for all 10 standard energies. The routine opens the file *\$EGRET_PROGRAMS/sequence/ scale.factor* and looks for an entry for the viewing period being analyzed. If it does not find an entry, it uses the value for the last entry in the table and it prints a message to that effect together with the value it is using. The scale factors are used to remove preliminary scaling so that the final value is absolute.

The viewing period residual diffuse and the portion of the Phase 1-3 diffuse maps for the same section of sky (produced in the previous step) are read for each energy interval. Both ratio analyses that were discussed in §2.1.2 are done. In this routine, the variance of the ratio of the summed intensities does not make the assumption that the error in the standard map is small. If at a given energy range, *vp_int* is the diffuse flux map and *vp_exp* is the corresponding exposure map, and likewise *std_int* and *std_exp* are the intensity and exposure maps for the standard phase 1-3 maps, then

$$\text{var}(\text{ratio}) = \text{ratio}^2 * \left\{ \frac{\sum_{15^\circ} [\text{vp_int}/\text{vp_exp}]}{\sum_{15^\circ} [\text{vp_int}]^2} + \frac{\sum_{15^\circ} [\text{std_int}/\text{std_exp}]}{\sum_{15^\circ} [\text{std_int}]^2} \right\} \quad (6)$$

For the 10 standard energy analysis, the ratio of the summed intensities seems much more stable due to the low statistics. This IDL routine prompts the user to see if plots are desired for the Gaussian fits and the radial and axial cut distributions. These plots did not appear to be useful since the Gaussian approach was not working well and so this option was not used to save analysis time.

The results from the IDL procedures for the > 100 MeV and the 10 standard energies are written to the screen and are also written in a file named *vpxxxx.results* in the subdirectories *VPxxxx*. In addition a line with the 10 energy values and their uncertainties are appended to a summary file named 'std.table' in the current directory. This file will be automatically created when the first period is analyzed.

2.3 Viewing Period Selection

The last full gas exchange occurred just prior to the start of Viewing Period 4280. Two viewing periods later in Phase 5 of the mission, EGRET began operating in narrow angle mode. Moreover, the EGRET high voltage pulsers were disabled during some viewing periods where there were no high priority targets. Table 2 lists the active periods along with the dates and times as well as the accumulated running time in days given for the midpoint of the viewing period. All viewing periods in Table 2 were used for this scale factor analysis although the short periods often have poor statistics.

Table 2. Summary of Active Viewing Periods Since the Last Gas Fill

VPN	Start Date	Start TJD	End TJD	Dur. Days	Accum Days
4280	09/07/95	9967.6	9980.5	11.9	6.5
4290	09/20/95	9980.6	9987.6	7.0	16.4
5010	10/03/95	9993.6	10007.5	14.0	26.9
5020	10/17/95	10007.6	10021.6	14.0	40.9
5070	11/28/95	10049.6	10059.0	9.4	52.6
5075	12/08/95	10059.0	10065.6	6.6	60.6
5080	12/14/95	10065.6	10071.6	6.0	66.9
5090	12/20/95	10071.7	10084.6	12.9	76.4
5100	01/02/96	10084.6	10087.6	2.9	84.3
5105	01/05/96	10087.6	10098.6	11.1	91.3
5110	01/16/96	10098.7	10112.6	14.0	103.8
5115	01/30/96	10112.7	10119.6	7.0	114.3
5130	02/06/96	10119.6	10126.6	7.0	121.3
5150	02/20/96	10133.7	10147.6	14.0	131.8
5170	03/05/96	10147.6	10160.6	13.0	145.3
5161	03/18/96	10160.6	10163.6	3.0	153.3
5165	03/21/96	10163.7	10176.6	12.9	161.3
5185	04/03/96	10176.6	10196.6	20.0	177.7
5190	04/23/96	10196.6	10210.6	14.0	194.7
5204	05/21/96	10224.6	10231.6	7.0	205.2
5210	05/28/96	10231.6	10245.5	13.9	215.7
5220	06/11/96	10245.6	10248.6	3.0	224.1
5260	07/30/96	10294.6	10308.6	14.0	232.6
5270	08/13/96	10308.6	10315.6	7.0	243.1
5280	08/20/96	10315.6	10322.6	7.0	250.1
5295	08/27/96	10322.6	10332.6	9.9	258.6
5300	09/06/96	10332.6	10359.6	27.0	277.0
5310	10/03/96	10359.7	10371.6	11.9	296.5
6011	10/15/96	10371.6	10385.6	13.9	309.4
6060	12/10/96	10427.7	10434.6	7.0	319.8
6070	12/17/96	10434.6	10440.6	6.0	326.3
6080	12/23/96	10440.7	10447.6	7.0	332.8
6090	12/30/96	10447.7	10455.7	8.0	340.3
6100	01/07/97	10455.7	10462.6	7.0	347.8
6105	01/14/97	10462.7	10469.6	7.0	354.8
6111	01/21/97	10469.7	10476.6	7.0	361.8
6161	02/18/97	10497.7	10525.6	28.0	379.3

Table 2. Continued

VPN	Start Date	Start TJD	End TJD	Dur. Days	Accum Days
6178	04/09/97	10547.6	10553.6	6.0	396.3
6215	06/17/97	10616.6	10623.6	7.0	402.8
6235	07/15/97	10644.6	10651.6	7.0	409.8
6250	08/05/97	10665.6	10679.6	14.0	420.3
6151	08/19/97	10679.6	10686.5	7.0	430.8
6270	09/02/97	10693.6	10700.5	7.0	437.8
6300	09/23/97	10714.6	10728.6	14.0	448.3
6311	11/03/97	10755.6	10763.6	8.0	459.3
7010	11/11/97	10763.7	10770.6	7.0	466.8
7020	11/18/97	10770.6	10777.6	7.0	473.8
7080	12/30/97	10812.6	10819.6	7.0	480.8
7091	01/06/98	10819.7	10826.6	7.0	487.8
7100	01/13/98	10826.7	10834.6	7.9	495.3
7110	01/21/98	10834.6	10840.6	6.0	502.2
7155	03/20/98	10892.7	10899.6	6.9	508.7
7165	03/27/98	10899.7	10905.8	6.1	515.2
7170	04/14/98	10917.6	10925.6	8.0	522.2
7210	05/15/98	10948.6	10952.6	4.0	528.2
7225	05/22/98	10955.6	10960.6	5.0	532.7
7245	07/07/98	11001.6	11015.6	14.0	542.2
7287	09/22/98	11078.6	11081.6	2.9	550.7
7289	10/13/98	11099.6	11120.6	21.0	562.6
8010	12/01/98	11148.6	11155.6	7.0	576.6
8020	12/08/98	11155.6	11162.7	2.1	581.2
8065	01/19/99	11197.6	11204.7	6.0	585.2
8067	01/26/99	11204.7	11211.6	7.0	591.7
8160	05/11/99	11309.6	11323.6	14.0	602.2
829	09/14/99	11435.6	11449.6	14.0	616.2
8339	11/18/99	11500.6	11505.6	5.0	625.7
9085	01/25/00	11568.6	11575.6	7.0	631.7
9100	02/08/00	11582.7	11597.7	14.0	642.2
9111	02/23/00	11597.7	11604.6	7.0	652.7
9150	04/04/00	11638.6	11645.6	7.0	659.7
9160	04/11/00	11645.6	11652.7	7.0	666.7
9175	04/18/00	11652.7	11659.6	6.9	673.7
9185	04/25/00	11659.6	11673.7	14.1	684.2
9195	05/09/00	11673.7	11691.0	17.3	699.9

3 Functional Behavior of the Scale Factors

The EGRET performance has varied with time since each gas fill. The time dependence is also a function of energy being a stronger function of time at low energies where the secondary tracks tend to be short and most influenced by inefficient decks. Given the efficiency measurements at each energy for all of the viewing periods listed in Table 2, an attempt was made to find an overall smooth function that describes both the time and energy dependences. The expectation is that the function would smooth out statistical fluctuations that could be rather large, and in addition to smooth other random systematic effects.

Two approaches were tried. In one, an attempt was made to fit the time variation of each of the 10 standard energy bins to an exponential decay function of time. It was hoped that the coefficients of each fit could be found to smoothly vary with energy. This approach was difficult at low and high energies because the statistics were poor. Instead, the energy dependence was observed to be rather well represented by linear function when plotted against $\log E$ for each viewing period. A quadratic fit in the same coordinate system was also tried, but the resulting linear and second order coefficients were found to be highly correlated and this approach was abandoned. The adopted functional fit to the energy dependence was then

$$\text{eff}(E, t) = \text{eff}_{100}(t) + \nu(t) * \log(E/100) \quad (7)$$

where E is measured in MeV. Figure 1 shows a sample of the energy variation for viewing periods that include all of the observations of the strong pulsars, Vela, Crab, and Geminga, since the last gas refill. The fits shown on these plots are for the global model discussed later. The parameters of the fits for all of the viewing periods are given in Table 3 along with reduced χ^2 values.

The time dependence of the two fit parameters, $\text{eff}_{100}(t)$ and $\nu(t)$ is shown in Figures 2 and 3. In these plots, an arbitrary systematic uncertainty of 10% has been added in quadrature to the uncertainties given in Table 3. Three distinct regions are apparent, especially in Figure 1 indicated by the vertical dotted lines, that resulted from the failure of Spark Chamber #2 on day 454, and from the partial gas refill that was done on day 572. The solid line in Figure 2 is a fit to an exponential function

$$\text{eff}_{100}(t) = N * \exp[-(t - t_0)/c] \quad (8)$$

The time constant, c , was determined from zone 1 and used in the other two zones while the normalization, N , was fitted in all three zones. In Figure 3, the solid line is a linear fit of the form

$$\nu(t) = a * (t - t_0) + b \quad (9)$$

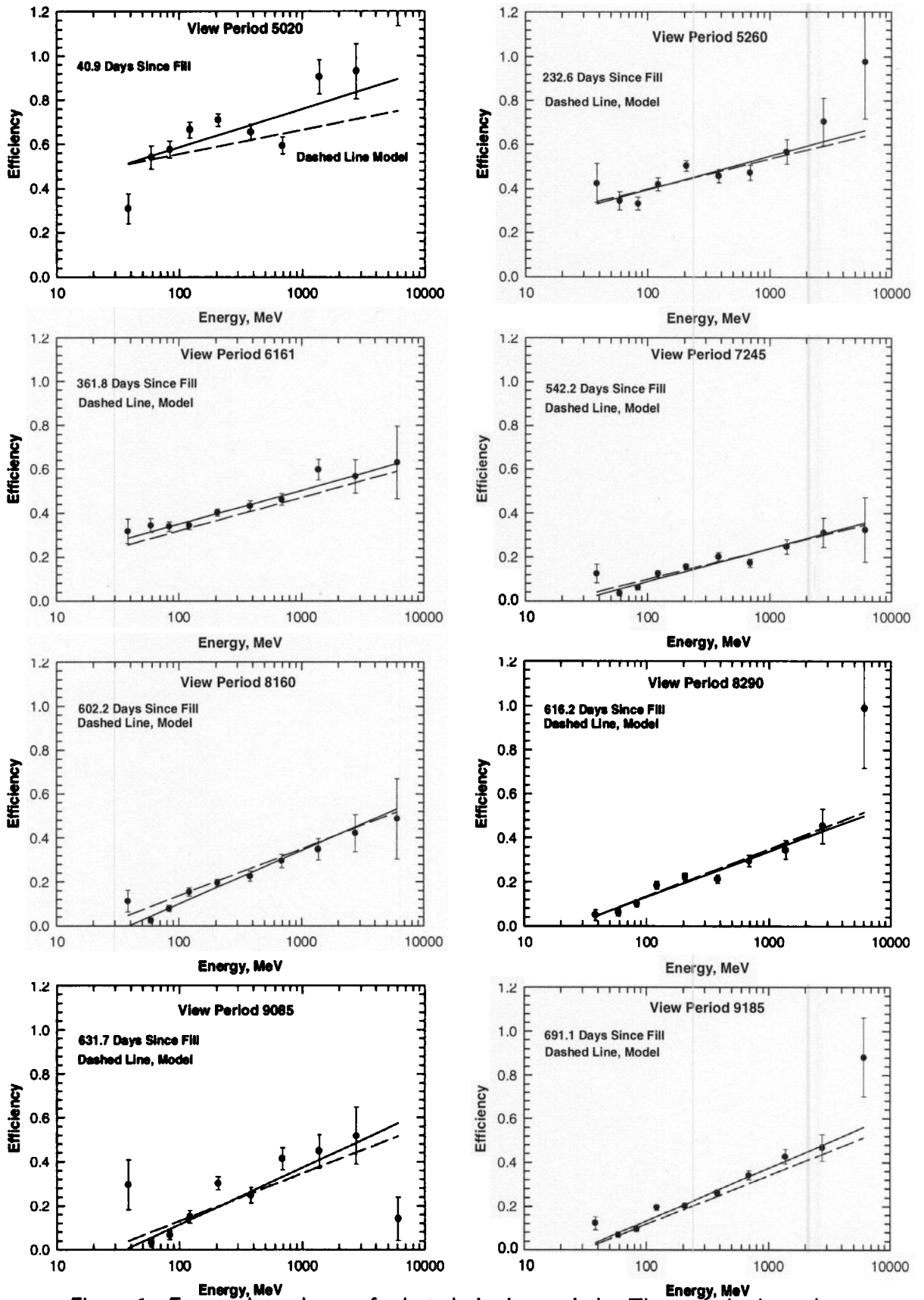


Figure 1. Energy dependence of selected viewing periods. The periods shown here are the pulsar observations since the last gas refill.

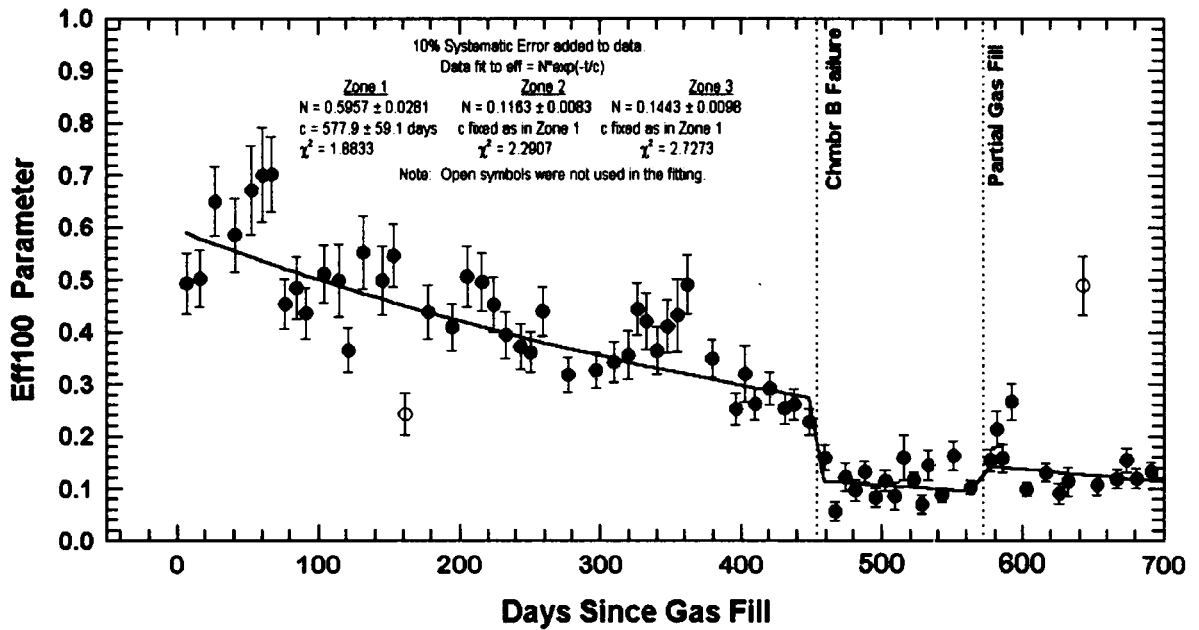


Figure 2. Parameter Eff_{100} for each viewing period since the last gas fill.

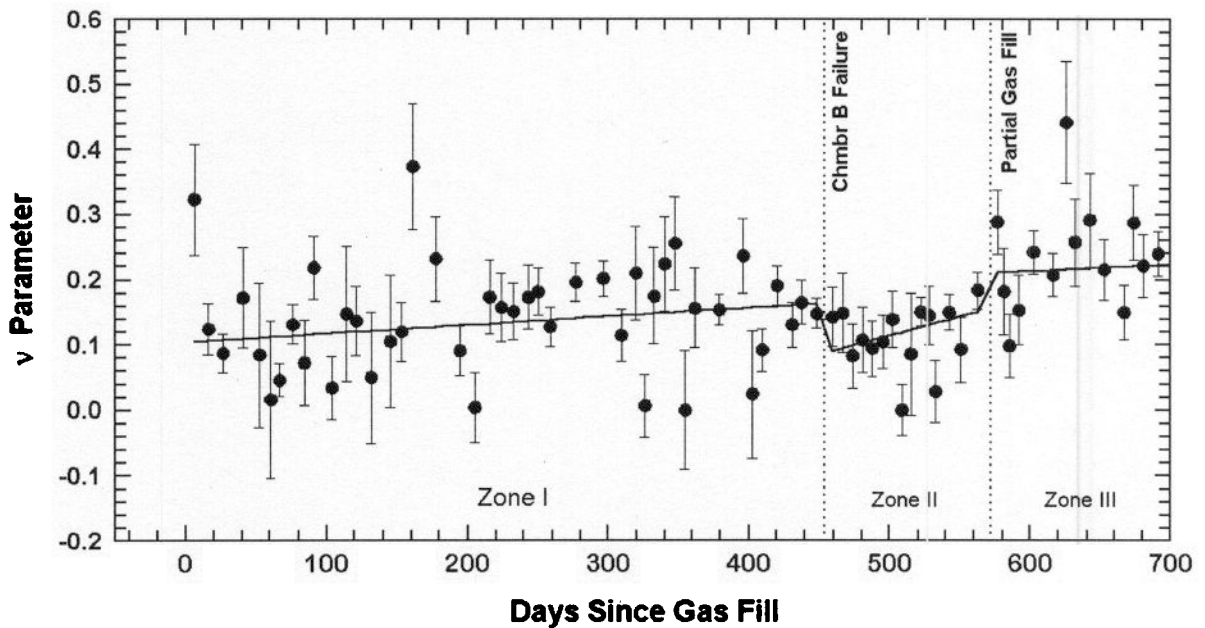


Figure 3. The v parameter is the coefficient of the $\log(E/100)$ in the energy fits of efficiency in each viewing period. An additional 10% systematic error has been added in quadrature to the statistical error on all points. A linear fit of the form $v = a \cdot (t - t_0) + b$ was made in each zone delineated by the dotted lines.

Zone 1, $t_0 = 0$ days	Zone 2, $t_0 = 454$ days	Zone 3, $t_0 = 572$ days
$a = (1.336 \pm 0.615) \times 10^4 \text{ day}^{-1}$	$a = (5.87 \pm 4.35) \times 10^4 \text{ day}^{-1}$	$a = (9.49 \pm 35.44) \times 10^5 \text{ day}^{-1}$
$b = 0.1040 \pm 0.0181$	$b = 0.08695 \pm 0.03067$	$b = 0.2105 \pm 0.0289$
$\chi^2 = 1.865$	$\chi^2 = 1.627$	$\chi^2 = 1.705$

Table 3. Viewing Period Energy Fits

VPN	Time Days	eff_{100}	δeff_{100}	ν	$\delta\nu$	χ_{red}^2
4280	6.5	0.4938	0.0306	0.3232	0.0789	1.6938
4290	16.4	0.5032	0.0200	0.1243	0.0380	3.5681
5010	26.9	0.6499	0.0155	0.0873	0.0283	1.7604
5020	40.9	0.5862	0.0387	0.1728	0.0754	4.6769
5070	52.6	0.6715	0.0536	0.0846	0.1101	2.1551
5075	60.6	0.7008	0.0580	0.0161	0.1201	1.7247
5080	66.9	0.7023	0.0137	0.0459	0.0242	0.5536
5090	76.4	0.4543	0.0138	0.1315	0.0274	1.4792
5100	84.3	0.4854	0.0341	0.0724	0.0651	0.7617
5105	91.3	0.4370	0.0212	0.2182	0.0432	1.1928
5110	103.8	0.5116	0.0224	0.0341	0.0473	0.8152
5115	114.3	0.4989	0.0481	0.1481	0.1026	2.2693
5130	121.3	0.3654	0.0230	0.1371	0.0518	0.7430
5150	131.8	0.5527	0.0435	0.0505	0.1003	1.7782
5170	145.3	0.4992	0.0431	0.1053	0.1002	2.2324
5161	153.3	0.5466	0.0244	0.1204	0.0441	1.0744
5165	161.3	0.2424	0.0324	0.3739	0.0890	3.9677
5185	177.7	0.4391	0.0263	0.2318	0.0606	2.3508
5190	194.7	0.4098	0.0163	0.0907	0.0371	0.5745
5204	205.2	0.5067	0.0272	0.0043	0.0537	0.6334
5210	215.7	0.4962	0.0234	0.1737	0.0538	0.8874
5220	224.1	0.4529	0.0262	0.1578	0.0503	0.8314
5260	232.6	0.3953	0.0210	0.1516	0.0410	1.9546
5270	243.1	0.3725	0.0234	0.1734	0.0456	1.5079
5280	250.1	0.3617	0.0157	0.1817	0.0306	0.8074
5295	258.6	0.4403	0.0146	0.1278	0.0273	1.6207
5300	277.0	0.3182	0.0102	0.1959	0.0212	1.9181
5310	296.5	0.3270	0.0093	0.2017	0.0184	0.4554
6011	309.4	0.3423	0.0191	0.1144	0.0387	1.8901
6060	319.8	0.3561	0.0299	0.2102	0.0685	1.0346
6070	326.3	0.4444	0.0216	0.0068	0.0484	0.3200
6080	332.8	0.4209	0.0331	0.1750	0.0720	1.0190
6090	340.3	0.3642	0.0282	0.2239	0.0683	1.0229
6100	347.8	0.4117	0.0282	0.2554	0.0673	0.9307
6105	354.8	0.4333	0.0542	0.0000	0.0909	
6111	361.8	0.4913	0.0264	0.1563	0.0588	0.6294
6161	379.3	0.3497	0.0085	0.1539	0.0176	0.6467

Table 3. Continued

VPN	Time Days	eff_{100}	δeff_{100}	ν	$\delta\nu$	χ^2_{red}
6178	396.3	0.2522	0.0182	0.2363	0.0518	0.5645
6215	402.8	0.3198	0.0439	0.0245	0.0975	2.6528
6235	409.8	0.2619	0.0157	0.0921	0.0315	0.9659
6250	420.3	0.2919	0.0117	0.1908	0.0227	2.5836
6151	430.8	0.2537	0.0161	0.1312	0.0325	1.5822
6270	437.8	0.2614	0.0145	0.1651	0.0292	1.1395
6300	448.3	0.2273	0.0084	0.1482	0.0173	1.0174
6311	459.3	0.1593	0.0175	0.1429	0.0432	1.2386
7010	466.8	0.0571	0.0177	0.1487	0.0593	5.5720
7020	473.8	0.1226	0.0227	0.0829	0.0490	1.8847
7080	480.8	0.0975	0.0178	0.1071	0.0490	1.8155
7091	487.8	0.1330	0.0157	0.0942	0.0414	0.9405
7100	495.3	0.0832	0.0160	0.1043	0.0395	2.8682
7110	502.2	0.1159	0.0164	0.1394	0.0409	1.5041
7155	508.7	0.0864	0.0253	0.0000	0.0385	
7165	515.2	0.1597	0.0403	0.0856	0.0930	1.6859
7170	522.2	0.1178	0.0071	0.1510	0.0159	0.5916
7210	528.2	0.0704	0.0177	0.1452	0.0430	2.2064
7225	532.7	0.1458	0.0246	0.0283	0.0474	1.2049
7245	542.2	0.0889	0.0098	0.1503	0.0231	2.7239
7287	550.7	0.1639	0.0216	0.0930	0.0494	0.6176
7289	562.6	0.1037	0.0075	0.1838	0.0214	0.9513
8010	576.6	0.1547	0.0141	0.2885	0.0403	0.4036
8020	581.2	0.2140	0.0271	0.1820	0.0634	0.2411
8065	585.2	0.1593	0.0209	0.0982	0.0478	0.9353
8067	591.7	0.2667	0.0223	0.1535	0.0505	0.7055
8160	602.2	0.0999	0.0089	0.2422	0.0235	1.7093
8290	616.2	0.1312	0.0110	0.2070	0.0255	2.2803
8339	625.7	0.0918	0.0176	0.4421	0.0820	0.8579
9085	631.7	0.1146	0.0251	0.2575	0.0621	5.7102
9100	642.2	0.4903	0.0276	0.2917	0.0660	1.2236
9111	652.7	0.1081	0.0164	0.2152	0.0406	2.4450
9150	666.6	0.1195	0.0140	0.1502	0.0391	0.9526
9160	673.6	0.1558	0.0169	0.2875	0.0504	1.1858
9175	680.6	0.1203	0.0145	0.2214	0.0421	1.2364
9185	691.1	0.1338	0.0103	0.2395	0.0255	3.4182
9195	706.8	0.1310	0.0112	0.2012	0.0291	2.4661

Table 4a. Summary of Eff_{100} Fit Parameters

Zone	t_0 days	N	δN	c days	δc days	χ^2_{red}
1	0	0.5957	0.0281	577.9	59.1	1.8833
2	454	0.1163	0.0083	577.9	59.1	2.2907
3	572	0.1443	0.0098	577.9	59.1	2.7273

Table 4b. Summary ν Fit Parameters

Zone	t_0 days	a day ⁻¹	δa day ⁻¹	b	δb	χ^2_{red}
1	0	1.336×10^4	0.615×10^4	0.1040	0.0181	1.865
2	454	5.87×10^4	4.35×10^4	0.08695	0.03067	1.627
3	572	9.49×10^5	3.54×10^4	0.2105	0.0289	1.705

made in each of the three zones. The fitted parameters of equations 8 and 9 are summarized in Tables 4a and 4b.

The modeled efficiency is then obtained from equation 7 with equations 8 and 9

$$\text{eff}(E, t) = N * \exp[-(t - t_0)/c] + [a * (t - t_0) + b] * \log(E/100) \quad (10)$$

with the parameters of Tables 4a and 4b. The parameters in this equation are relatively uncorrelated so that the estimated uncertainty is given by

$$\begin{aligned} \delta\text{eff}(E, t) = & \left\{ e^{-2(t-t_0)/c}(\delta N)^2 + [N e^{-(t-t_0)/c}(\delta c)]^2 \right. \\ & \left. + [(t - t_0)(\delta a)\log(E/100)]^2 + [(\delta b)\log(E/100)]^2 \right\}^{1/2} \end{aligned} \quad (11)$$

Table 5 lists the model efficiency factors computed from equation 11 for the 10 standard energy regions from the time of the last gas refill. A factor of 1.00 corresponds to the instrument performance when it was calibrated before flight. The likelihood program automatically constructs scale factors for other energy regions, notably the wide intervals based on the 10 standard energy values. Relative uncertainties calculated using equation 11 are given in Table 6.

Figures 4a, 4b, 4c, and 4d show the data and the model fits for the 10 standard energy regions. As mentioned earlier, a 10 % systematic uncertainty has been added to the statistical errors. Below 50 MeV and above 1000 MeV, the statistics are quite poor. The χ^2 values shown on these plots generally are reasonable. Arbitrarily adding a larger systematic error would reduce them further.

Table 5. Model Derived Efficiency Factors

View Period	Energy, MeV									
	30 50	50 70	70 100	100 150	150 300	300 500	500 1000	1000 2000	2000 4000	4000 10000
4280	0.545	0.565	0.581	0.598	0.622	0.650	0.677	0.709	0.740	0.776
4290	0.535	0.555	0.571	0.588	0.613	0.641	0.668	0.700	0.732	0.768
5010	0.524	0.544	0.560	0.578	0.603	0.631	0.659	0.691	0.724	0.760
5020	0.509	0.530	0.546	0.564	0.590	0.619	0.647	0.680	0.713	0.750
5070	0.498	0.518	0.535	0.553	0.579	0.609	0.637	0.670	0.704	0.742
5075	0.490	0.511	0.527	0.546	0.572	0.602	0.630	0.664	0.698	0.736
5080	0.483	0.505	0.522	0.540	0.566	0.596	0.625	0.659	0.693	0.732
5090	0.474	0.496	0.513	0.532	0.558	0.588	0.618	0.652	0.687	0.726
5100	0.467	0.488	0.506	0.525	0.551	0.582	0.612	0.646	0.681	0.720
5105	0.460	0.482	0.499	0.518	0.545	0.576	0.606	0.641	0.676	0.716
5110	0.449	0.471	0.488	0.508	0.535	0.566	0.597	0.632	0.668	0.708
5115	0.439	0.461	0.479	0.499	0.527	0.558	0.589	0.625	0.661	0.701
5130	0.433	0.455	0.473	0.493	0.521	0.553	0.584	0.620	0.656	0.697
5150	0.423	0.446	0.464	0.484	0.513	0.545	0.576	0.613	0.649	0.691
5170	0.412	0.435	0.453	0.474	0.502	0.535	0.567	0.604	0.641	0.683
5161	0.405	0.428	0.447	0.467	0.496	0.529	0.561	0.599	0.636	0.679
5165	0.398	0.422	0.441	0.461	0.490	0.524	0.556	0.594	0.632	0.674
5185	0.385	0.409	0.428	0.449	0.478	0.512	0.545	0.584	0.622	0.666
5190	0.371	0.395	0.415	0.436	0.466	0.501	0.534	0.574	0.613	0.657
5204	0.363	0.387	0.407	0.429	0.459	0.494	0.528	0.567	0.607	0.652
5210	0.355	0.380	0.399	0.421	0.452	0.487	0.522	0.562	0.602	0.647
5220	0.348	0.373	0.393	0.416	0.447	0.482	0.517	0.557	0.597	0.643
5260	0.342	0.367	0.387	0.410	0.441	0.477	0.512	0.552	0.593	0.639
5270	0.334	0.360	0.380	0.403	0.434	0.471	0.506	0.547	0.588	0.634
5280	0.329	0.355	0.375	0.398	0.430	0.466	0.502	0.543	0.584	0.631
5295	0.323	0.349	0.370	0.392	0.425	0.461	0.497	0.539	0.580	0.628
5300	0.310	0.336	0.358	0.381	0.413	0.451	0.487	0.530	0.572	0.620
5310	0.297	0.324	0.345	0.369	0.402	0.440	0.477	0.520	0.564	0.613
6011	0.288	0.315	0.337	0.361	0.395	0.433	0.471	0.514	0.558	0.608
6060	0.281	0.309	0.331	0.355	0.389	0.428	0.466	0.510	0.554	0.604
6070	0.277	0.305	0.327	0.351	0.385	0.425	0.463	0.507	0.551	0.602
6080	0.273	0.301	0.323	0.347	0.382	0.421	0.459	0.504	0.549	0.600
6090	0.268	0.296	0.319	0.343	0.378	0.418	0.456	0.501	0.546	0.597
6100	0.263	0.292	0.314	0.339	0.374	0.414	0.453	0.498	0.543	0.595
6105	0.259	0.288	0.310	0.335	0.370	0.411	0.449	0.495	0.541	0.592
6111	0.255	0.283	0.306	0.331	0.367	0.407	0.446	0.492	0.538	0.590
6161	0.244	0.273	0.297	0.322	0.358	0.399	0.439	0.485	0.532	0.585
6178	0.235	0.264	0.287	0.313	0.350	0.391	0.432	0.479	0.526	0.580

Table 5. Continued

View Period	Energy, MeV									
	30 50	50 70	70 100	100 150	150 300	300 500	500 1000	1000 2000	2000 4000	4000 10000
6215	0.231	0.260	0.284	0.310	0.347	0.389	0.429	0.477	0.524	0.578
6235	0.227	0.257	0.280	0.307	0.343	0.386	0.426	0.474	0.522	0.576
6250	0.221	0.251	0.275	0.301	0.338	0.381	0.422	0.470	0.519	0.573
6151	0.215	0.245	0.270	0.296	0.334	0.377	0.418	0.467	0.515	0.571
6270	0.211	0.242	0.266	0.293	0.331	0.374	0.416	0.465	0.513	0.569
6300	0.206	0.236	0.261	0.288	0.326	0.370	0.412	0.461	0.510	0.566
6311	0.078	0.094	0.108	0.123	0.144	0.168	0.191	0.218	0.245	0.276
7010	0.074	0.092	0.106	0.122	0.144	0.169	0.193	0.221	0.250	0.282
7020	0.071	0.090	0.104	0.121	0.144	0.170	0.195	0.225	0.254	0.288
7080	0.068	0.087	0.103	0.120	0.143	0.171	0.197	0.228	0.259	0.294
7091	0.065	0.085	0.101	0.119	0.143	0.172	0.199	0.231	0.264	0.300
7100	0.062	0.083	0.099	0.118	0.143	0.173	0.202	0.235	0.269	0.307
7110	0.059	0.080	0.098	0.117	0.143	0.174	0.204	0.238	0.273	0.312
7155	0.056	0.078	0.096	0.116	0.143	0.175	0.206	0.242	0.277	0.318
7165	0.053	0.076	0.095	0.115	0.143	0.176	0.208	0.245	0.282	0.324
7170	0.050	0.074	0.093	0.114	0.144	0.177	0.210	0.248	0.286	0.330
7210	0.048	0.072	0.092	0.113	0.144	0.178	0.212	0.251	0.290	0.335
7225	0.046	0.071	0.091	0.113	0.144	0.179	0.213	0.253	0.293	0.339
7245	0.042	0.068	0.089	0.112	0.144	0.181	0.216	0.258	0.300	0.347
7287	0.038	0.065	0.087	0.111	0.144	0.182	0.219	0.262	0.305	0.355
7289	0.033	0.062	0.084	0.109	0.144	0.184	0.223	0.268	0.314	0.365
8010	0.055	0.095	0.126	0.161	0.210	0.266	0.320	0.384	0.447	0.519
8020	0.054	0.093	0.125	0.160	0.209	0.265	0.319	0.383	0.447	0.519
8065	0.053	0.092	0.124	0.159	0.208	0.264	0.319	0.382	0.446	0.519
8067	0.051	0.091	0.122	0.157	0.207	0.263	0.318	0.382	0.446	0.518
8160	0.048	0.088	0.120	0.155	0.204	0.261	0.316	0.380	0.444	0.517
8290	0.044	0.084	0.116	0.152	0.202	0.259	0.314	0.378	0.443	0.516
8339	0.041	0.082	0.114	0.150	0.200	0.257	0.312	0.377	0.442	0.516
9085	0.040	0.080	0.113	0.148	0.198	0.256	0.312	0.377	0.442	0.516
9100	0.037	0.078	0.110	0.146	0.196	0.254	0.310	0.375	0.441	0.515
9111	0.034	0.075	0.108	0.144	0.194	0.253	0.309	0.374	0.440	0.514
9150	0.031	0.072	0.105	0.141	0.192	0.250	0.307	0.373	0.439	0.514
9160	0.029	0.070	0.103	0.140	0.191	0.249	0.306	0.372	0.438	0.513
9175	0.027	0.069	0.102	0.138	0.189	0.248	0.305	0.371	0.438	0.513
9185	0.025	0.066	0.100	0.136	0.188	0.247	0.304	0.370	0.437	0.513
9195	0.021	0.063	0.096	0.133	0.185	0.244	0.302	0.369	0.436	0.512

Table 6. Relative Uncertainties of Model Derived Efficiency Factors

View Period	Energy, MeV									
	30 50	50 70	70 100	100 150	150 300	300 500	500 1000	1000 2000	2000 4000	4000 10000
4280	0.053	0.050	0.048	0.047	0.046	0.046	0.047	0.049	0.052	0.055
4290	0.053	0.050	0.048	0.047	0.046	0.046	0.047	0.049	0.052	0.055
5010	0.053	0.050	0.048	0.047	0.046	0.046	0.047	0.049	0.052	0.055
5020	0.054	0.051	0.049	0.047	0.046	0.046	0.047	0.050	0.052	0.056
5070	0.055	0.051	0.049	0.047	0.046	0.046	0.048	0.050	0.053	0.057
5075	0.055	0.052	0.049	0.048	0.047	0.047	0.048	0.050	0.053	0.057
5080	0.056	0.052	0.050	0.048	0.047	0.047	0.048	0.051	0.054	0.057
5090	0.056	0.052	0.050	0.048	0.047	0.047	0.049	0.051	0.054	0.058
5100	0.057	0.053	0.050	0.049	0.047	0.048	0.049	0.052	0.055	0.058
5105	0.058	0.053	0.051	0.049	0.048	0.048	0.049	0.052	0.055	0.059
5110	0.059	0.054	0.052	0.050	0.048	0.049	0.050	0.053	0.056	0.060
5115	0.060	0.055	0.052	0.050	0.049	0.049	0.051	0.054	0.057	0.061
5130	0.061	0.056	0.053	0.051	0.049	0.050	0.051	0.054	0.057	0.062
5150	0.062	0.057	0.054	0.052	0.050	0.050	0.052	0.055	0.058	0.063
5170	0.064	0.058	0.055	0.053	0.051	0.051	0.053	0.056	0.060	0.064
5161	0.065	0.059	0.056	0.053	0.052	0.052	0.054	0.057	0.061	0.065
5165	0.066	0.060	0.057	0.054	0.052	0.053	0.054	0.058	0.061	0.066
5185	0.069	0.062	0.058	0.055	0.054	0.054	0.056	0.059	0.063	0.068
5190	0.071	0.064	0.060	0.057	0.055	0.056	0.058	0.061	0.065	0.070
5204	0.073	0.066	0.061	0.058	0.056	0.057	0.059	0.062	0.066	0.071
5210	0.075	0.067	0.062	0.059	0.057	0.058	0.060	0.064	0.068	0.073
5220	0.077	0.068	0.063	0.060	0.058	0.059	0.061	0.065	0.069	0.074
5260	0.078	0.069	0.065	0.061	0.059	0.059	0.062	0.066	0.070	0.075
5270	0.080	0.071	0.066	0.062	0.060	0.060	0.063	0.067	0.072	0.077
5280	0.082	0.072	0.067	0.063	0.061	0.061	0.064	0.068	0.073	0.078
5295	0.084	0.073	0.068	0.064	0.062	0.062	0.065	0.069	0.074	0.079
5300	0.088	0.077	0.070	0.066	0.064	0.064	0.067	0.071	0.076	0.082
5310	0.092	0.080	0.073	0.068	0.066	0.066	0.069	0.074	0.079	0.085
6011	0.095	0.082	0.075	0.070	0.067	0.068	0.071	0.076	0.081	0.087
6060	0.098	0.084	0.077	0.071	0.068	0.069	0.073	0.078	0.083	0.089
6070	0.100	0.085	0.078	0.072	0.069	0.070	0.073	0.079	0.084	0.090
6080	0.102	0.087	0.079	0.073	0.070	0.071	0.074	0.080	0.085	0.092
6090	0.104	0.088	0.080	0.074	0.071	0.072	0.075	0.081	0.086	0.093
6100	0.106	0.090	0.081	0.075	0.072	0.073	0.076	0.082	0.088	0.094
6105	0.108	0.091	0.082	0.076	0.073	0.074	0.077	0.083	0.089	0.095
6111	0.110	0.092	0.083	0.077	0.073	0.075	0.078	0.084	0.090	0.097
6161	0.115	0.096	0.086	0.079	0.075	0.077	0.081	0.087	0.093	0.100
6178	0.121	0.100	0.089	0.081	0.078	0.079	0.083	0.090	0.096	0.103

Table 6. Continued

View Period	Energy, MeV									
	30 50	50 70	70 100	100 150	150 300	300 500	500 1000	1000 2000	2000 4000	4000 10000
6215	0.123	0.101	0.090	0.082	0.078	0.080	0.084	0.091	0.097	0.104
6235	0.126	0.103	0.091	0.083	0.079	0.081	0.085	0.092	0.098	0.106
6250	0.129	0.105	0.093	0.085	0.080	0.082	0.087	0.094	0.100	0.108
6151	0.133	0.108	0.094	0.086	0.082	0.084	0.088	0.095	0.102	0.110
6270	0.136	0.109	0.096	0.087	0.083	0.085	0.089	0.097	0.104	0.111
6300	0.140	0.112	0.097	0.088	0.084	0.086	0.091	0.098	0.105	0.113
6311	0.196	0.115	0.079	0.070	0.089	0.118	0.142	0.165	0.184	0.201
7010	0.206	0.118	0.080	0.070	0.089	0.118	0.142	0.165	0.183	0.199
7020	0.218	0.121	0.081	0.070	0.090	0.119	0.143	0.165	0.183	0.199
7080	0.232	0.125	0.081	0.070	0.091	0.121	0.145	0.168	0.185	0.201
7091	0.249	0.130	0.082	0.070	0.093	0.124	0.149	0.171	0.188	0.204
7100	0.271	0.137	0.083	0.071	0.095	0.128	0.153	0.176	0.193	0.208
7110	0.294	0.143	0.084	0.071	0.098	0.132	0.158	0.181	0.198	0.213
7155	0.319	0.150	0.086	0.072	0.101	0.136	0.163	0.186	0.204	0.219
7165	0.348	0.158	0.087	0.072	0.104	0.141	0.168	0.192	0.209	0.225
7170	0.384	0.167	0.088	0.073	0.108	0.146	0.174	0.198	0.216	0.232
7210	0.419	0.175	0.090	0.073	0.111	0.151	0.180	0.204	0.222	0.238
7225	0.448	0.182	0.091	0.074	0.114	0.155	0.184	0.209	0.227	0.243
7245	0.519	0.198	0.093	0.075	0.119	0.163	0.194	0.219	0.237	0.253
7287	0.597	0.214	0.096	0.076	0.125	0.171	0.202	0.228	0.247	0.263
7289	0.735	0.240	0.100	0.079	0.133	0.182	0.214	0.241	0.260	0.276
8010	0.282	0.125	0.079	0.062	0.064	0.073	0.082	0.090	0.096	0.101
8020	0.289	0.126	0.079	0.062	0.064	0.074	0.082	0.090	0.096	0.102
8065	0.295	0.127	0.080	0.062	0.064	0.074	0.083	0.091	0.097	0.102
8067	0.308	0.129	0.080	0.062	0.065	0.075	0.084	0.092	0.098	0.104
8160	0.332	0.134	0.081	0.063	0.066	0.077	0.087	0.096	0.102	0.108
8290	0.375	0.141	0.082	0.063	0.069	0.082	0.093	0.102	0.109	0.115
8339	0.411	0.147	0.083	0.063	0.071	0.086	0.097	0.107	0.115	0.121
9085	0.437	0.151	0.083	0.064	0.073	0.089	0.101	0.111	0.119	0.125
9100	0.490	0.160	0.085	0.064	0.076	0.094	0.107	0.118	0.126	0.133
9111	0.554	0.170	0.086	0.065	0.080	0.100	0.114	0.126	0.135	0.142
9150	0.660	0.185	0.088	0.066	0.085	0.108	0.124	0.137	0.147	0.154
9160	0.723	0.194	0.090	0.067	0.089	0.113	0.130	0.143	0.153	0.161
9175	0.796	0.203	0.091	0.068	0.092	0.118	0.135	0.149	0.160	0.168
9185	0.924	0.218	0.093	0.069	0.097	0.125	0.144	0.159	0.170	0.178
9195	1.174	0.243	0.097	0.071	0.105	0.137	0.158	0.174	0.185	0.195

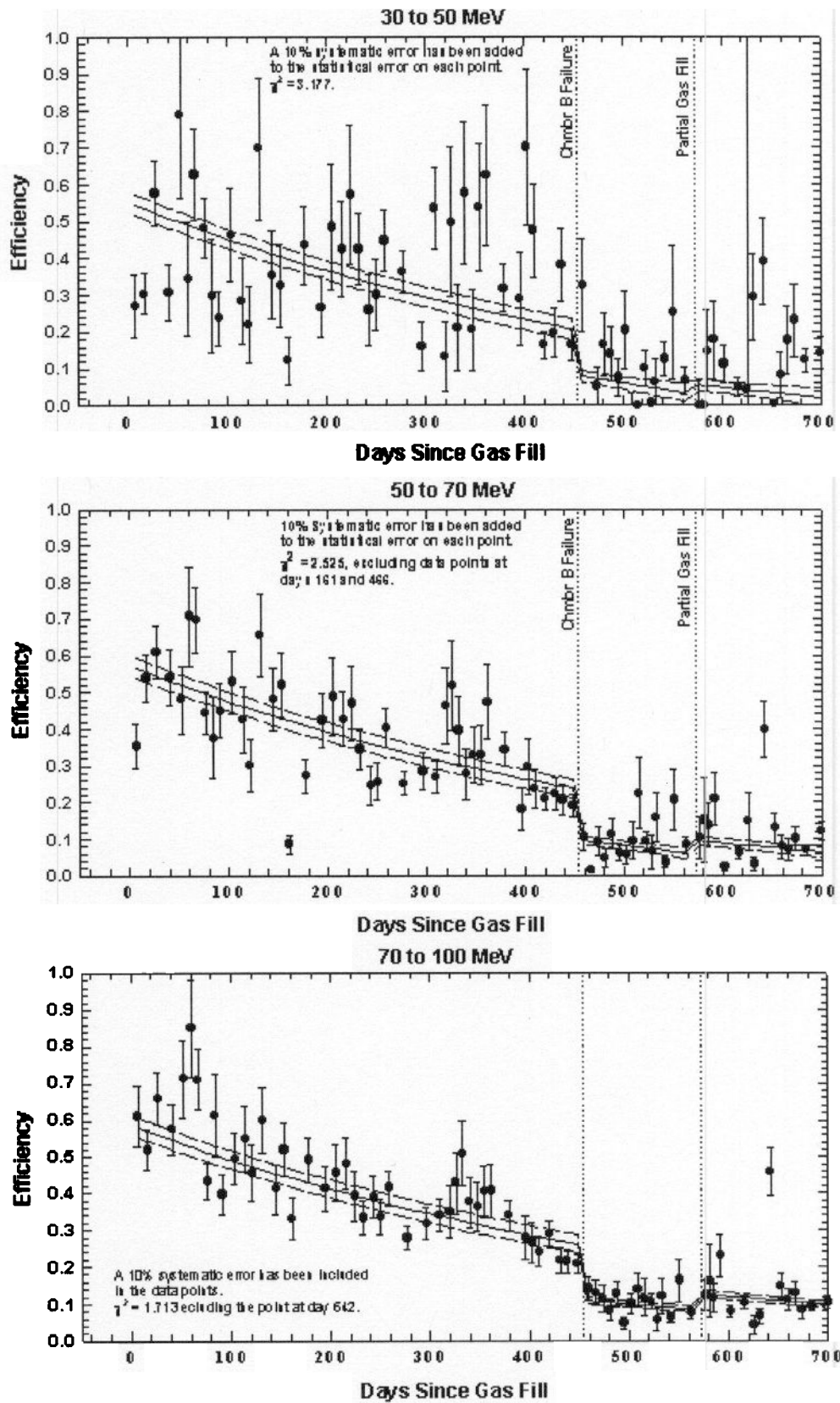


Figure 4a. Observed efficiency as a function of time for selected energies. Lines are the model fit and one standard deviation uncertainty.

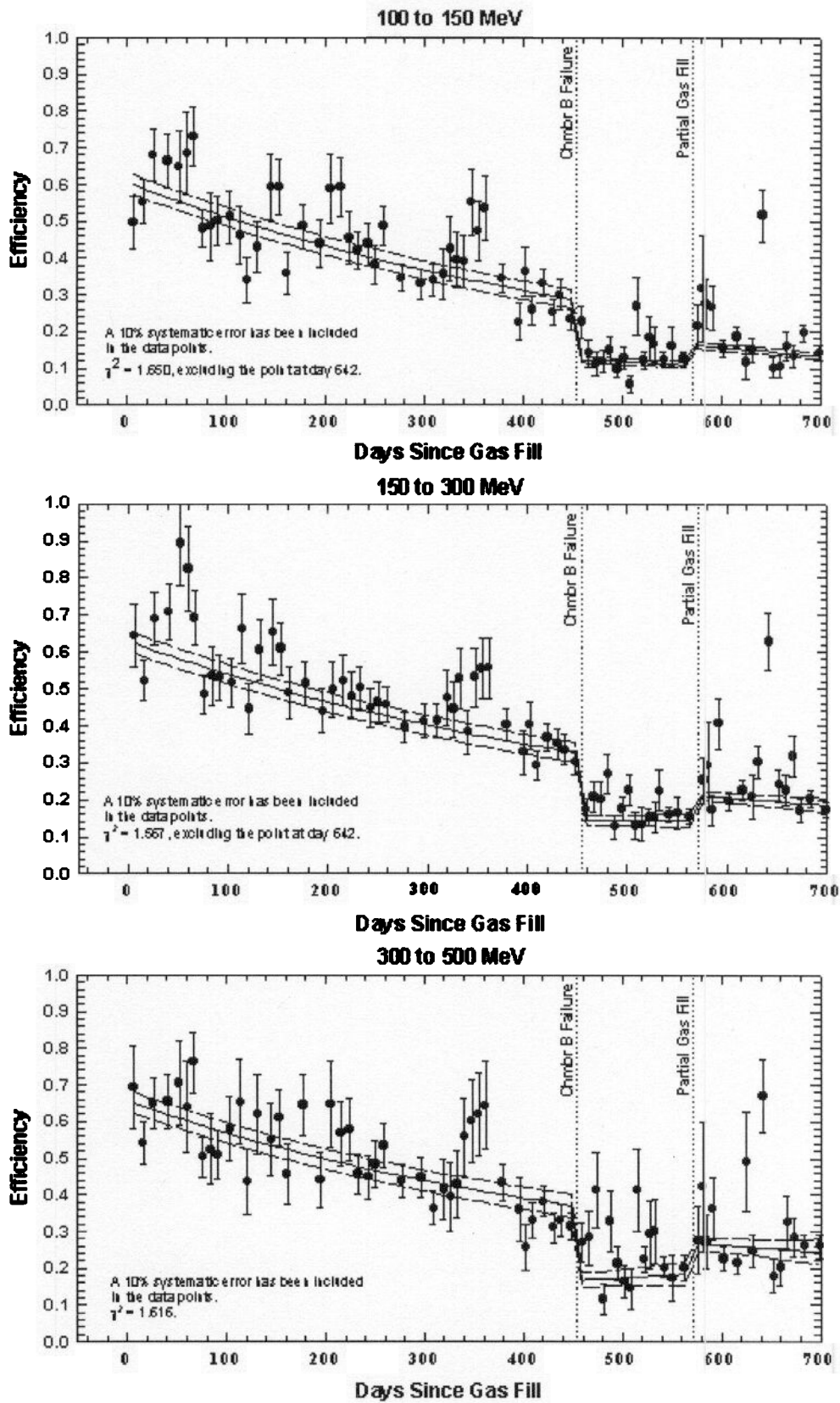


Figure 4b. Observed efficiency as a function of time for selected energies. Lines are the model fit and one standard deviation uncertainty.

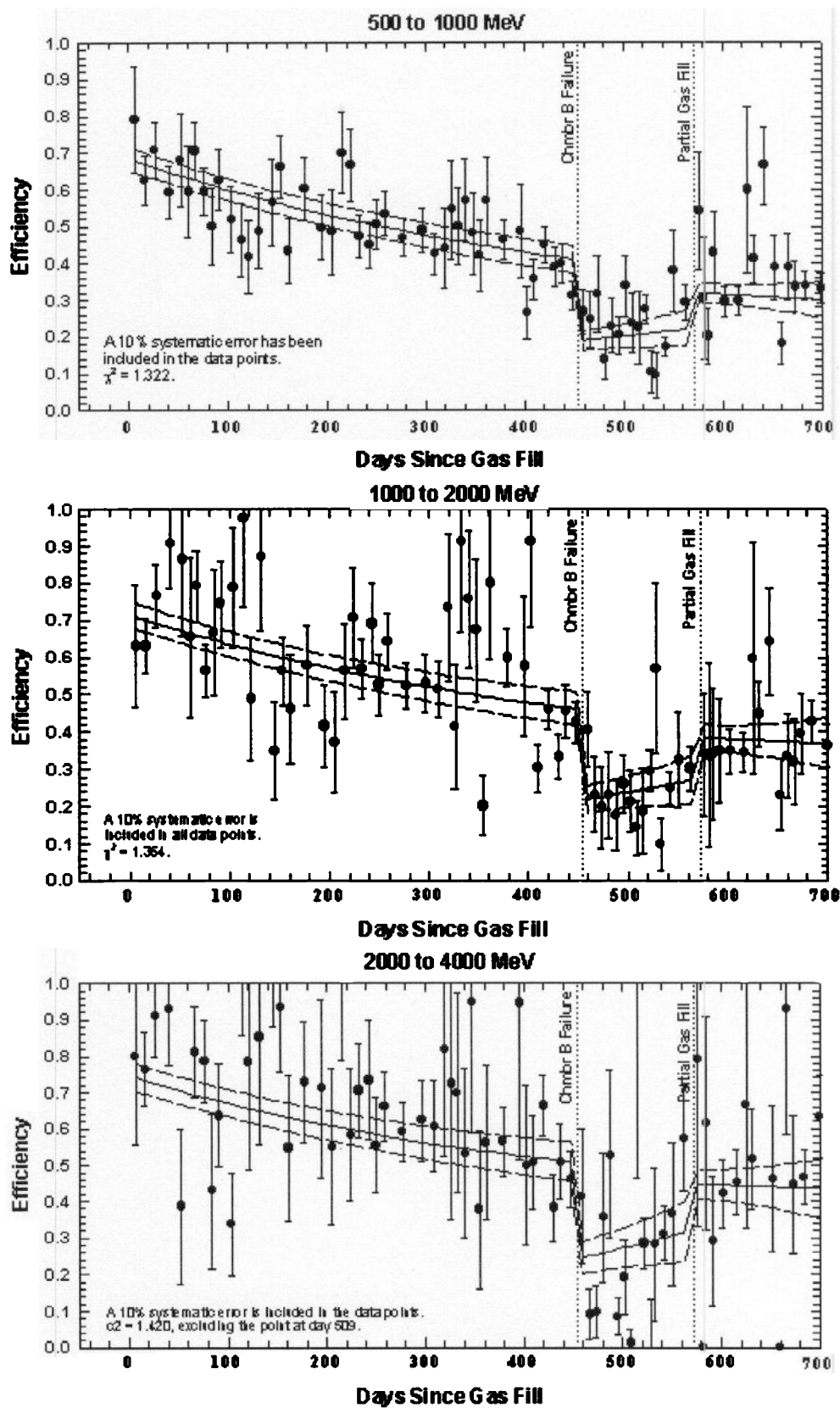


Figure 4c. Observed efficiency as a function of time for selected energies. Lines are the model fit and one standard deviation uncertainty

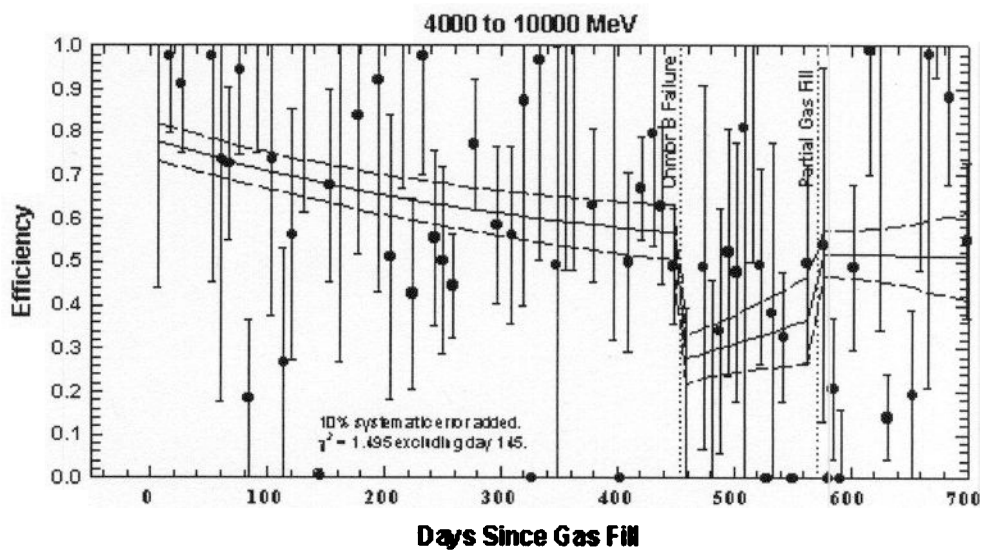


Figure 4d. Observed efficiency as a function of time for selected energies. Lines are the model fit and one standard deviation uncertainty.

4 Tests of the Model Efficiency Factors

Several viewing periods since the last gas fill were aimed in the vicinity of the three strong pulsars, Crab, Geminga, and Vela. Since these sources are believed to have constant intensity, they afford a means for assessing the model efficiency factors. Efficiency factors determined for these periods could be used directly without any need for modeling. However, other periods without strong sources are not always well determined. The model affords a method of smoothing and extrapolating the efficiencies and their uncertainties between viewing periods. The energy variation determined by the model (equations 10) was plotted in Figure 1 along with the data and the fit to the data for that period. The viewing periods shown in Figure 1 are the ones where the three strong pulsars were observed. The agreement between the model and the fit for each of those periods is quite good, both in terms of the value at 100MeV and slope.

Figures 5a,b,c compare the fluxes determined for the pulsar observation viewing periods with fluxes for the summed Phase 1-3 periods. Two panels are shown for each source and viewing period. The upper panel employed the model efficiencies, and the lower panel used efficiencies that were determined by the ratio of the residual maps as described in Section 2. The results shown in these figures are given as ratios between the flux to the Phase 1-3 for each of the 10 standard energy intervals. Notice that there is no significant departure from the desired value of one. Also notice that the results for the two sets of efficiencies are highly correlated. The use of model values rather than those directly observed does not impact the quality of the results. The uncertainties in these plots are statistical and they include the uncertainties in the efficiency factors.

The determined efficiency factor for energy $> 100\text{MeV}$ is a **b**-product of the method described in Section 2. Figure 6a shows the flux ratio between individual viewing periods with the flux from the Phase 1-3 summed map for energy $> 100\text{MeV}$. Here in the top panel, LIKE used the model values for the 10 standard energy intervals to generate a $> 100\text{MeV}$ value while the bottom panel used the directly observed efficiency. The weighted average ratio and its uncertainty is plotted for the Crab and Geminga sources. The agreement with the expected value of one is perhaps only questionable in the case of the model value for Geminga. LIKE uses a piecewise continuous power law when the effective efficiency for non standard energy bins are encountered. The Geminga spectrum perhaps is not well modeled by the LIKE algorithm. In addition, Geminga is fairly far off axis ($> 10^\circ$) for the narrow angle modes that were used in most of these observations and may contribute systematic errors that are not accounted for here. Figure 6b shows the $> 300\text{MeV}$ and $> 1000\text{MeV}$ LIKE results based on the model efficiencies. For these cases, direct determinations in the manner described in Section 2 were not done. The agreement is quite good for energies $> 300\text{MeV}$ and there a tendency for the fluxes to be too high at energies $> 1000\text{MeV}$, particularly for Geminga. The uncertainties in Figure 6 include the uncertainties in the efficiency factors.

Finally, Figure 7 compares spectra determined by SPECTRAL for the pulsar viewing periods. The dotted line in these plots is the spectrum obtained from the summed Phase

1-3 maps as a basis of comparison. For most cases, the agreement is within the statistical uncertainties. Viewing periods 7245 and to a lesser extent 6161 stand out as being problematic. No obvious explanation is known.

5 Conclusions

The efficiency values determined by equation 10 with the parameter values of Table 4 give reasonable agreement with the efficiency-corrected pulsar fluxes and spectra as compared to the Phase 1-3 summed map. The Phase 1-3 results involve corrections too whose effects are small compared to the corrections late in the mission. These have not been considered here.

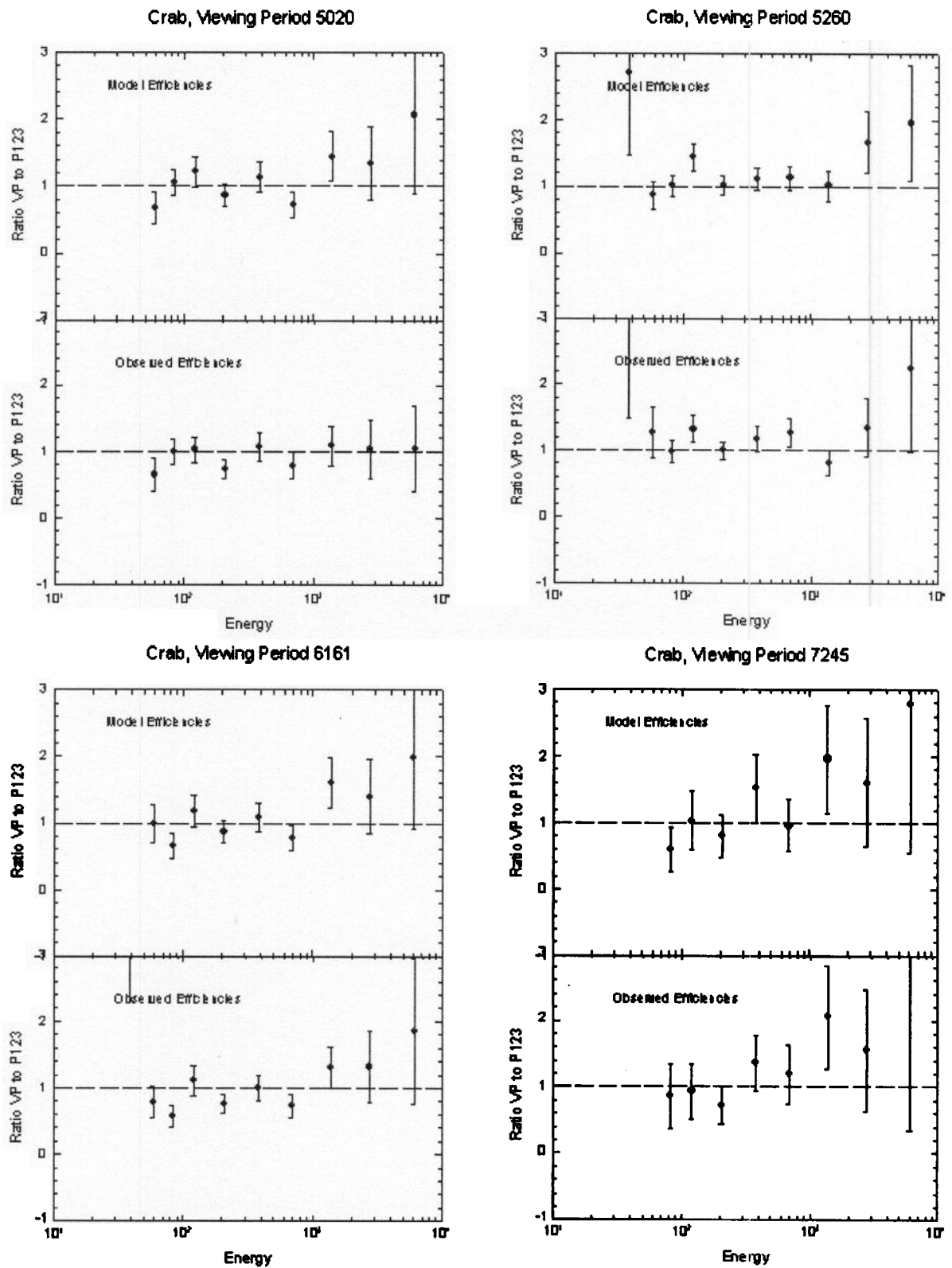


Figure 5a. Ratio of viewing period flux to the Phase 1-3 flux. The bottom panels use actual observed efficiencies (ratio of diffuse in the viewing period to the Phase 1-3 diffuse) and the top panels use the model efficiencies. Note the good agreement.

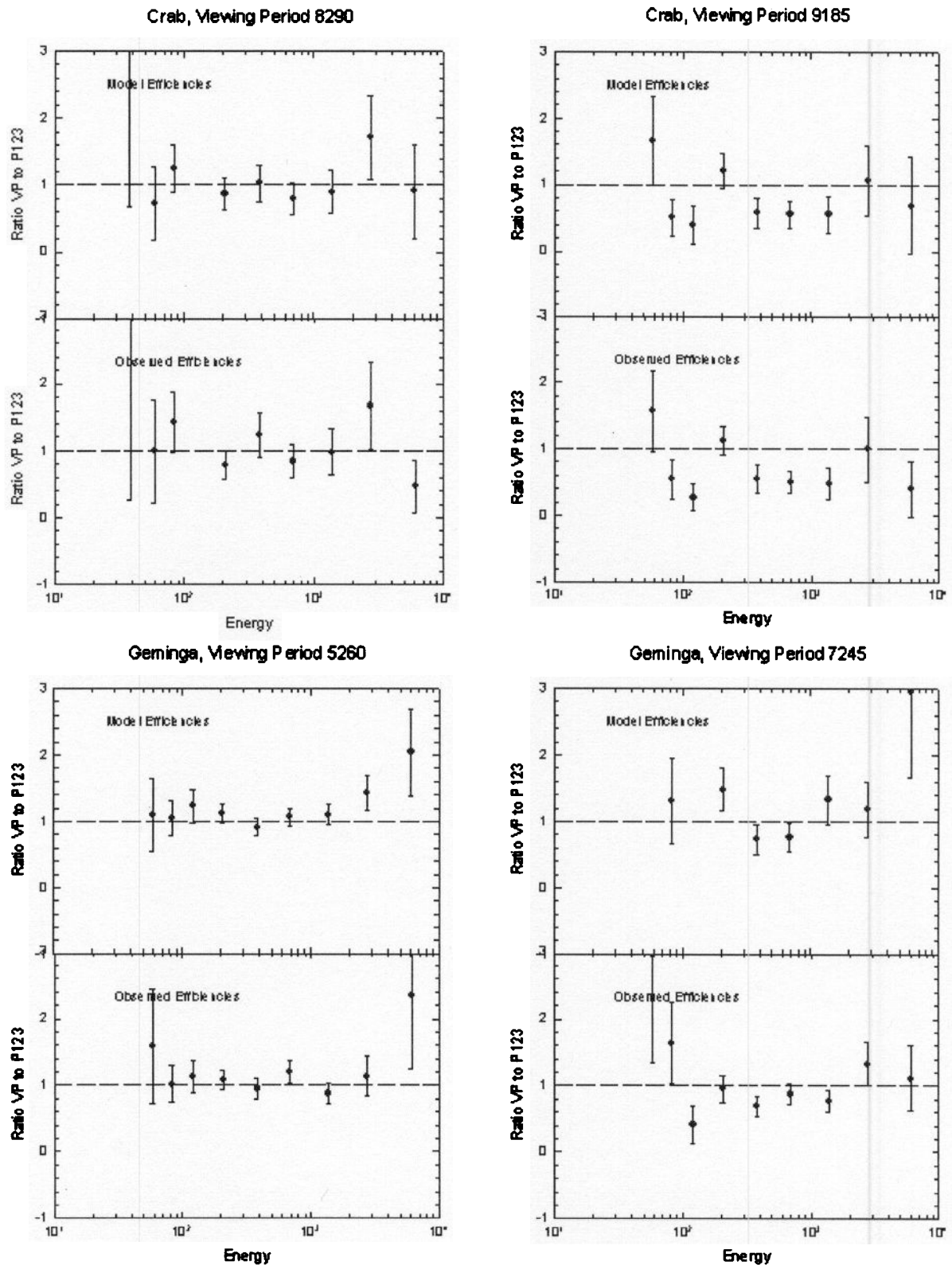
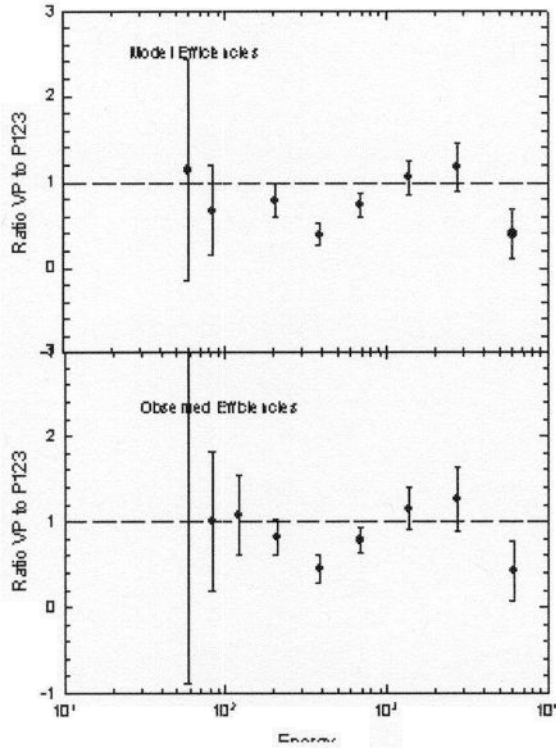
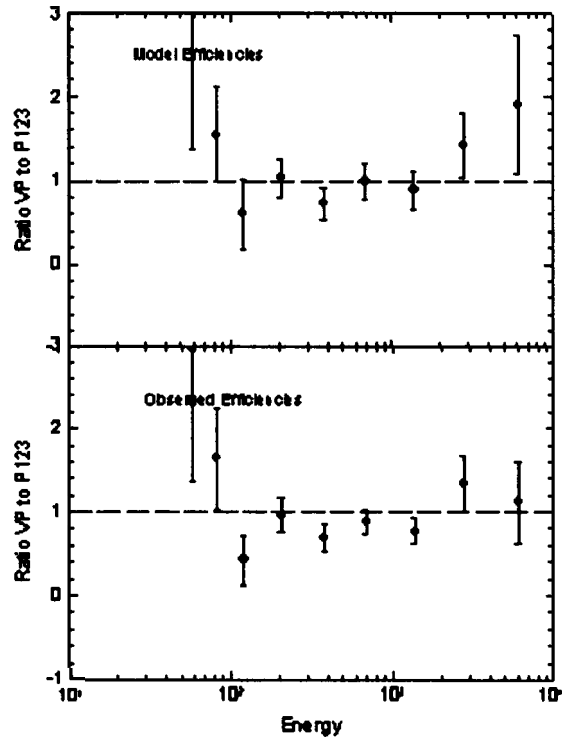


Figure 5b. Ratio of viewing period flux to the Phase 1-3 flux. The bottom panels use actual observed efficiencies (ratio of diffuse in the viewing period to the Phase 1-3 diffuse), and the top panels use the model efficiencies. Note the good agreement.

Geminga, Viewing Period 8160



Geminga, Viewing Period 9185



Vela, Viewing Period 9085

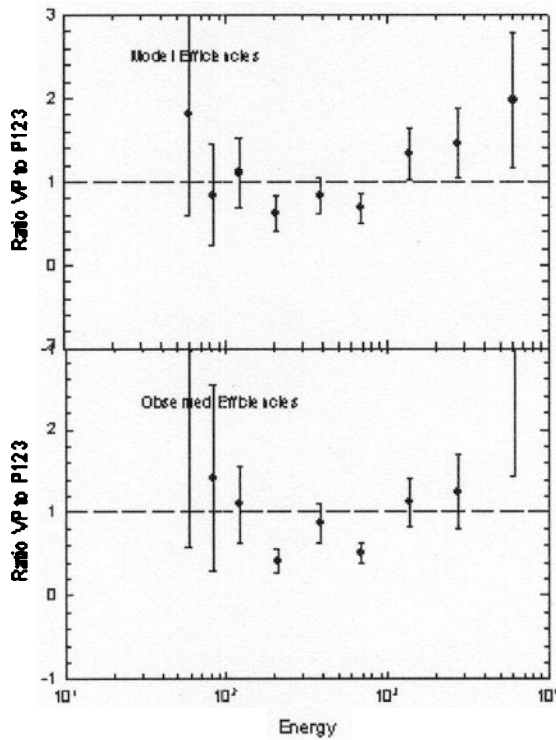


Figure 5c. Ratio of viewing period flux to the Phase 1-3 flux. The bottom panels use actual observed efficiencies (ratio of diffuse in the viewing period to the Phase 1-3 diffuse) and the top panels use the model efficiencies. Note the good agreement.

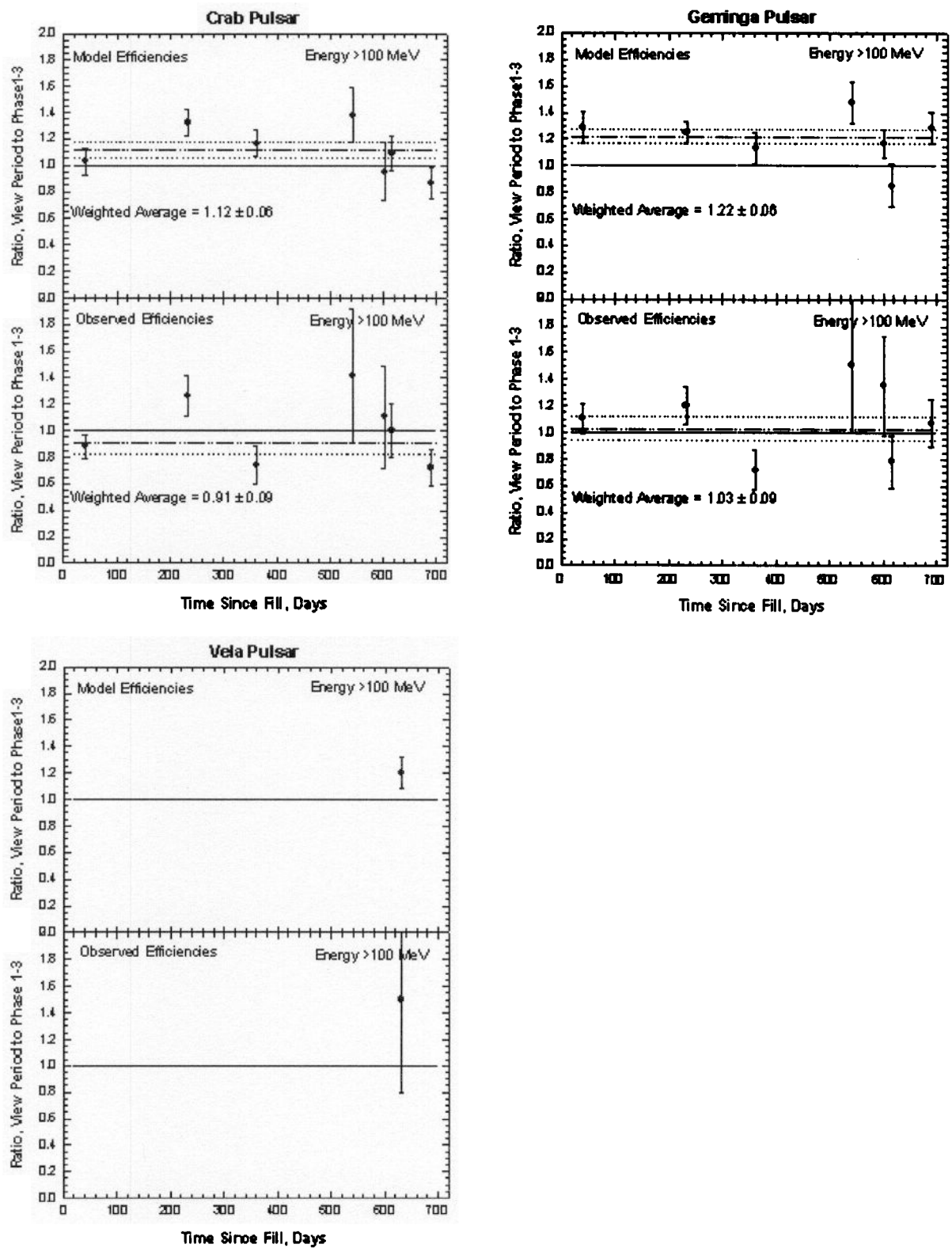


Figure 6a. Comparison of the >100 MeV flux for individual viewing periods with the flux observed for Phase 1 through 3. The upper panel is for the model efficiencies, and the lower panel for the efficiencies determined specifically for each period.

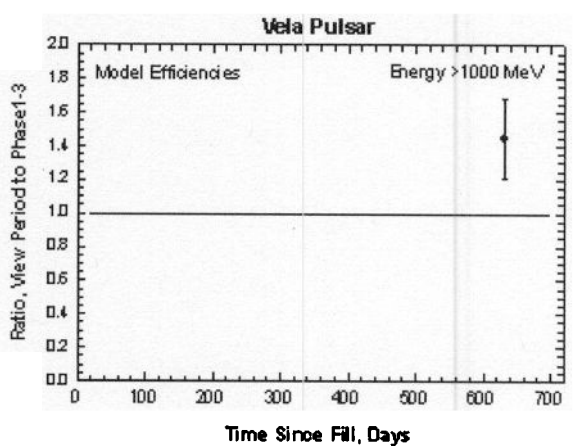
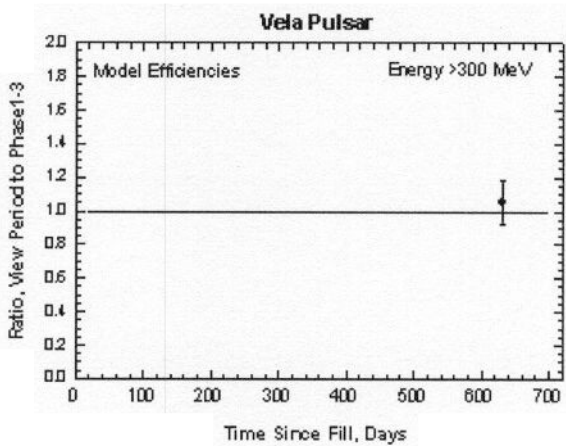
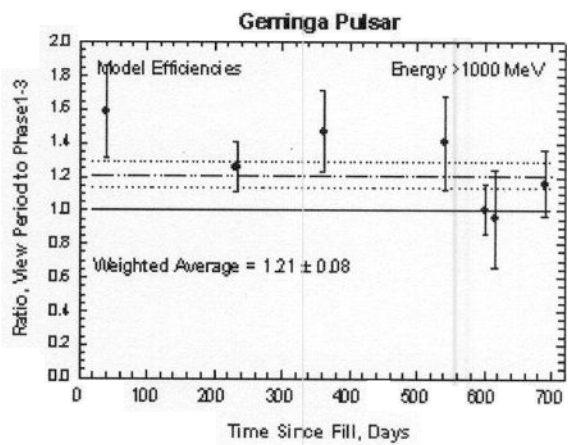
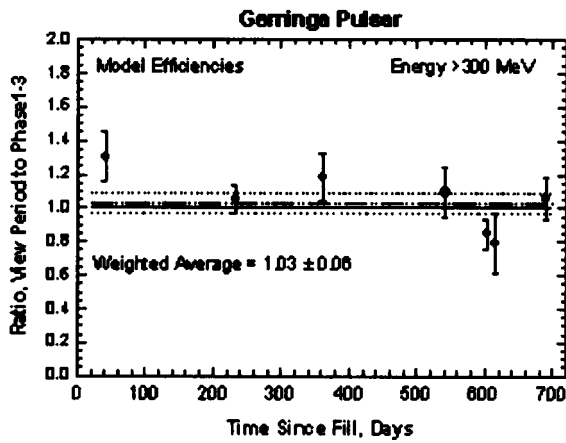
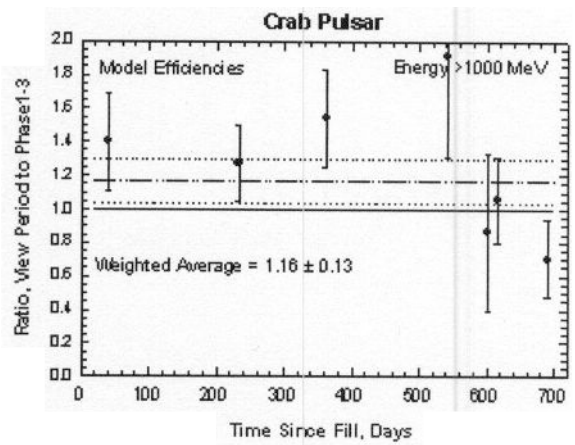
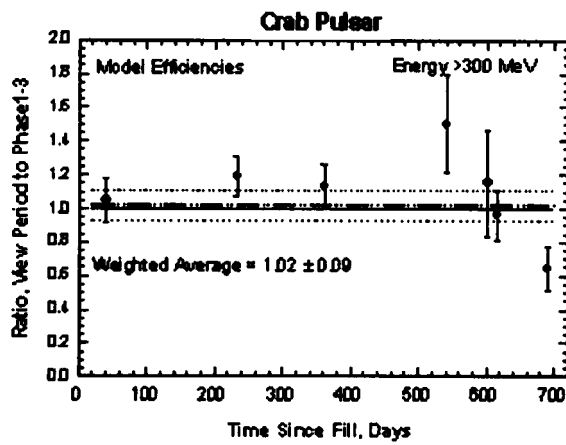


Figure 6b. Comparison of the >300 MeV (left) and >1000 MeV (right) fluxes for individual viewing periods with the Phase 1-3 fluxes. Model efficiencies based on the 10 standard energy efficiencies were used here. Wide energy band analysis was not done for the two energy ranges shown here.

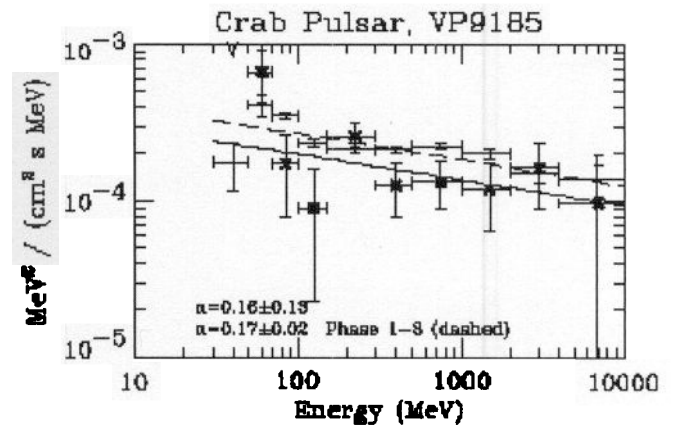
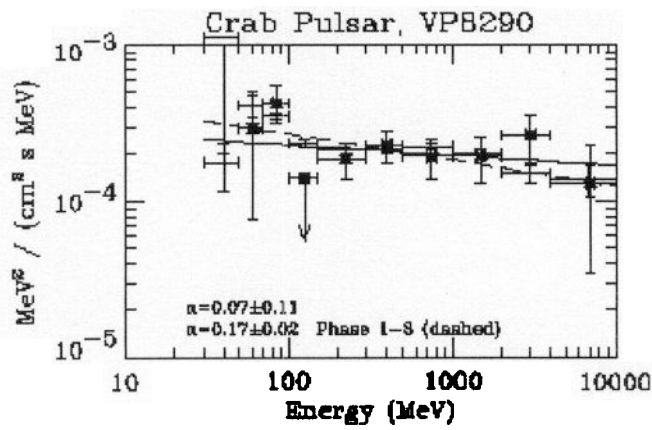
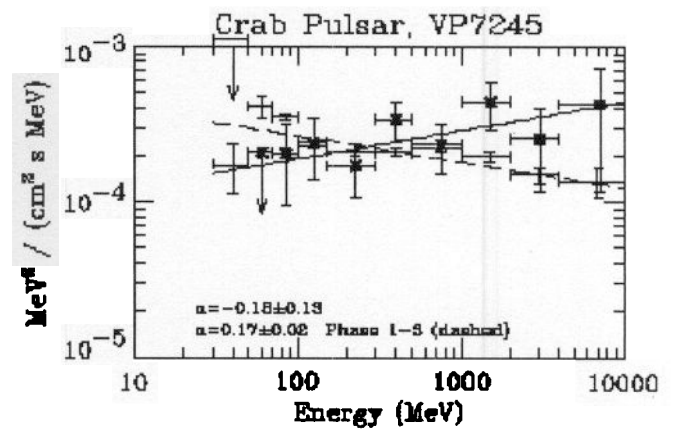
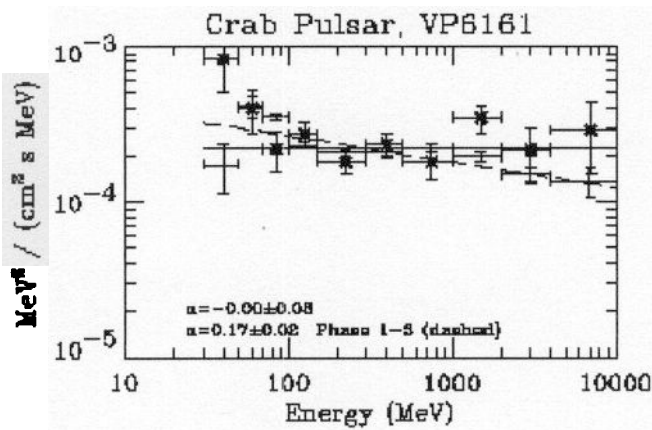
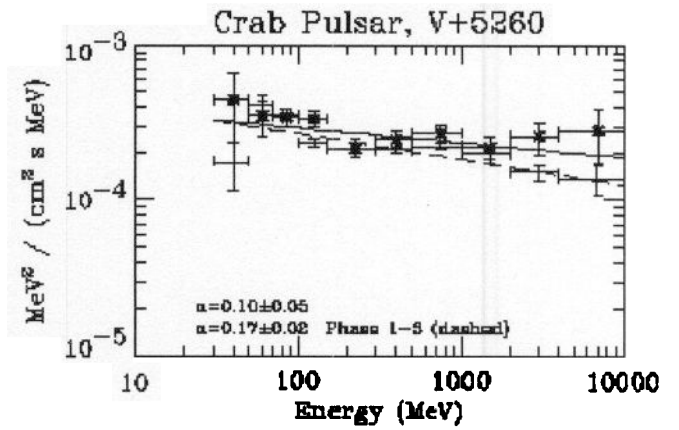
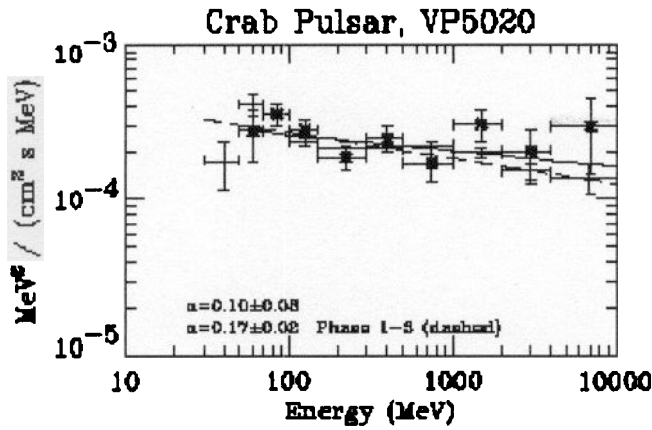


Figure 7a. Pulsar spectra since the last gas refill. The points show as asterisk are for the indicated viewing period. Points without symbol are for the summed Phase 1-3. The spectral indices are indicated in each panel.

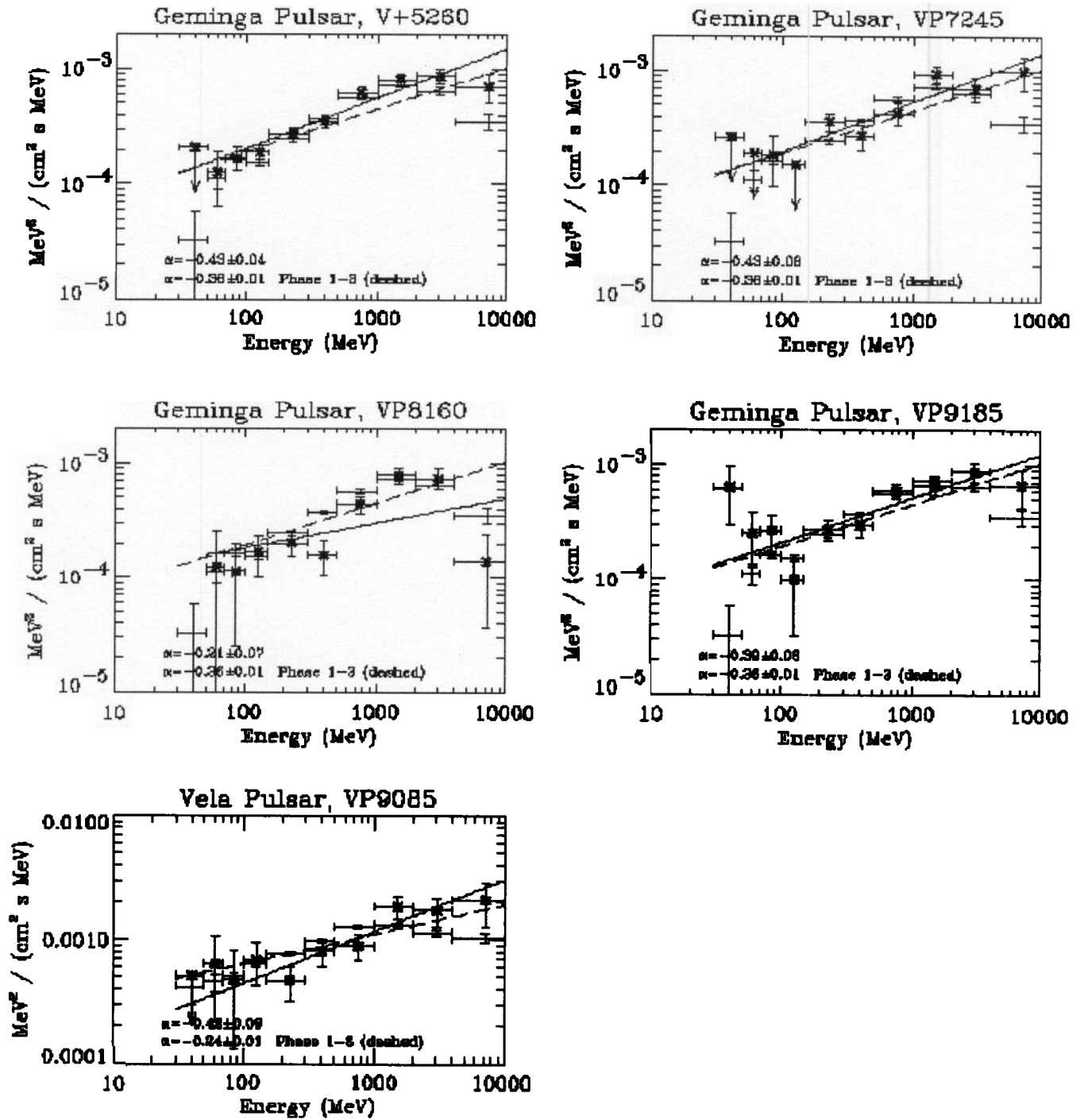


Figure 7b. Pulsar spectra since the last gas refill. The points show as asterisk are for the indicated viewing period. Points without symbol are for the summed Phase 1-3. The spectral indices are indicated in each panel.